Heartrate-Dependent Heartwave Biometric Identification with Thresholding-Based GMM-HMM Methodology

C.L.P. Lim, W.L. Woo, S.S. Dlay and Bin Gao

***Abstract*— This paper presents an adaptive heartrate dependent heartwave signal based biometric identification. A reliable and continuous heartwave extraction method featuring hybridized Discrete Waveform Transform method with heartrate adaptive QT and PR interval to perform comprehensive heartwave features extractions on more than 35,000 heartwave signal. The size of training data was determined and hybridized GMM-HMM classification method was used in the classification. Dynamic thresholding criterial incorporating user specific scores and heartrate were adopted. The identification process using dynamic thresholding criterial achieved a remarkable Receiver Operating Characteristic of 0.89 in True Positive Rate and an Equal Error Rate of 0.11.**

***Index Terms*— Discrete Wavelet Transform, QT Nomogram, Gaussian Mixture Model, Hidden Markov Model, ECG, Heartwave, electrocardiogram**

I. Introduction

THIS paper presents the use of individual heartwave signal as a biometric mode. Numerous research works have been established and have ascertained that heartwave signal indeed has the characteristic traits to be used as a biometric mode [1, 2]. Unlike other biometric modes mentioned, heartwave as biometric mode does not require sophisticated setup [3-7] for signal acquisitions. Heartwave signal can simply be acquired between two fingers electrodes.

With the rising of Internet-of-Things (IoT), there have been calls by government agencies for greater security in authentication and identification. Token based 2-Factor Authentication (2FA) technology mainly used in e-banking service is being explored to support pervasive advancement in cloud services and on-demands applications [8-11]. Heartwave as biometric mode has great potential to complement existing 2FA infrastructure for secured access to services and products through the means of wearable devices and smart connected systems. For example a reported work on using biometric to enhance transportation safety such as authenticated access to vehicle and detection of drowsiness via heartwave signal [12]. Apart from real-time IoT applications, with the rapid increase in elderly population, there are intense developments in tele-health systems to provide continuously monitoring on the well-being of the elderly [13]. Biometric based authentication and identification method for access to services allows medical personnel to respond to elderly needs reliably, securely and promptly.

Every individual has its own resting heartrate and maximum heartwave. At resting state, heart rate variation is at minimal and the heart rate of an individual can range from 50 bpm to as much as 180 bpm in accordance to the maximum heart rate equation of "220 bpm – age of an individual". The impetus of variations can be contributed by many factors such physiological activities, psychological related and pathological related issues. Even in resting, variation of the heartwave signal exists due to movement of the respiratory cage although the variation is minimal [14, 15]. Hence, as heartwave morphology varies according to heartrate and as a biometric mode, reliable extraction of heartwave features is essential.

The use of heartwave signal as biometric mode has aroused many research works with approaches such as KNN classifiers [16-18], LDA classifier [19], Support Vector Machine and Match Score Classifier [20] and Generative Model Classifier [21-23]. Unfortunately, all of the above works use ECG data that were obtained under resting condition where individual heartrate is not under physical duress. As mentioned, the morphology of an individual heartwave changes under different heartrate. One reported work [24] uses data comprises of heartwave signal under varied conditions of heartwave wellness. The work uses auto-correlation method to discard anomaly waveform of Premature Ventricular Contraction (PVC). PVC is a heart anomaly signal that occurs sporadically unlike the repetitive heartwave signal. Linear Discriminant is subsequently used to perform classification. Although under varied condition, the work does not use signals that are acquired under physical duress. In medical related fields, the works [21, 23, 25] use signal processing tools and Hidden Markov Model (HMM) to detect heartwave anomaly for individual with cardiac related problem. In those works, heartwaves of multiple individuals are concatenated as part of the HMM model for anomaly detection. The HMM model is thus not appropriate for individual classification and individual as individual heartwave morphologies vary across individual heart rate.

This paper presents a novel *heartrate-dependent* heartwave based biometric approach to perform identification. Importantly this work uses the full spectrum of individual

C.L.P. Lim, W.L. Woo S.S. Dlay and Bin Gao are currently with School of Electrical and Electronic Engineering, Newcastle University, England, United Kingdom. Corresponding author e-mail: w.l.woo@ncl.ac.uk.

heartwave variations acquired from individual under treadmill testing. To cater for heartwave morphological variations, the proposed architecture incorporated a heartrate dependent parameter to aid in the extraction of heartwave features. Equally important, the proposed architecture uses a combined GMM-HMM methodology with user specific thresholding criteria to address morphological variations to achieve a unique individual model that can be used for identification. See Fig. 1.

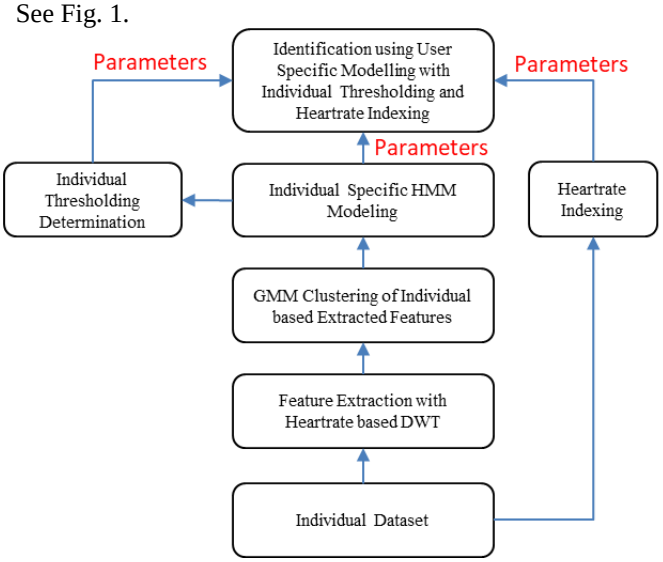

Fig.1. Proposed architecture

This paper is organized as follows: Section II presents the methodology in the extraction of heartwave features in particular to the full range of morphological heartwave variations in a user. Section III describes the data preparation with Section IV describing the proposed architecture of user specific GMM-HMM modelling. Section V covers architecture optimization with experimentation results. The paper concludes with recommendation and on-going development in Section VI.

II. Heartwave Data and Features Extraction

This work uses database from Physionet under ST Change dataset where it contains ECG signals of individuals acquired from ECG treadmill. In ECG treadmill acquisition, individual will start off in a resting state. In the treadmill session, the system will stress an individual physically at increasing intensity till an individual has reached it maximum heartrate. Thereafter, the individual will undergo a recovery phase till the heartrate returns to resting state. See Fig.2 for details.

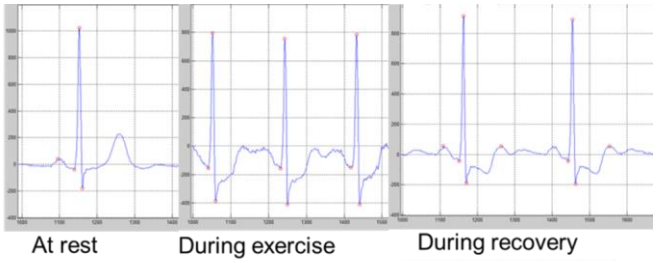

Fig.2. Different heartwave morphologies at different heartrates and after intense physical duress from an individual

In a recent work by [26], an adaptive threshold with principal component analysis (PCA) is used to perform heartwave feature extraction. The method uses Hilbert Transform for QRS-Complex detection. Thereafter PCA is used to determine the principal components from ordered eigenvectors. The drawback of the compared work is the inflexibility for heartwave signal under variable heartrate. At elevated heartrate, the periodic of T-Wave can reduce by as much as 40%. Thus a uniform data length will consist of overlapping heartwave signals at elevated heartrate which affects the eigenvectors for features discrimination.

To enable a successful extraction of heartwave features, the extraction uses a Discrete Waveform Transform (DWT) hybridized with heartrate related parameters of QT Interval and PR Interval to perform extraction of features related to P-Wave and T-Wave [27]. In elevated heartrate, period of T-Wave under intense physical duress can vary as much as 40% as compared T-Wave under normal heartrate. To enable detection peaks and valleys, a dynamic detection window that is proportion to heartrate is imposed about R-Peak to minimize incorrect detection of peaks and valleys in reconstructed DWT signal. This dynamic window also addresses sporadic peak noise contributed by signal electrode, motion artifacts and Premature Ventricular Contraction (PVC). In total, 11 features are detected. See Fig. 3 for details. DWT works by separating signals into different frequency bands where critical information at different scales can be easily qualified and quantified. Signal from DWT is decomposed into a coarse approximation and detail information. The decomposed coefficient can be used to determine temporal localization of the heartwave components such as the onset and offset of P-Wave, QRS-Wave complex and T-Wave.

Current reported work [28-32] have used DWT for feature extraction. However those work were trialed on databases whose individual heartwave signal were at resting state at heart rate of less than 100 bpm where the frequency for each heartwave feature was consistent. In the full range of heartrate from resting heartrate to maximum heartrate, each of the 11 heartwave features is a composition of multiple frequencies. The mentioned previous work which used single level coefficient, cannot be applied to variated heartwave signals under dynamic heartrate.

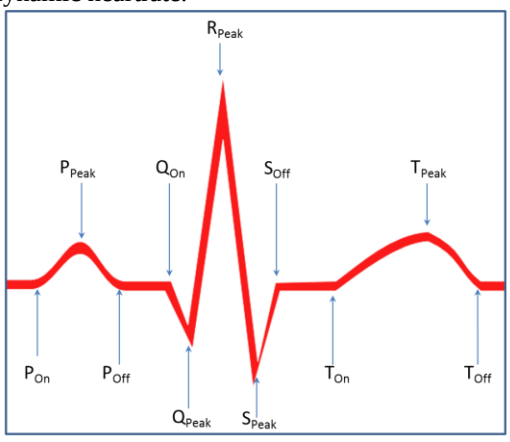

Fig.3. 11 heartwave features for classification

A. QRS-Complex Features Extraction

In the extraction of heartwave features in particular to R-Peak, Q-Peak and S-Peak, the method uses reconstructed signal comprises of details coefficient from Level 3, 4 and 5. The selection of levels is due to the frequency components that exist between 15Hz to 25Hz similar to the frequencies spectrum of QRS-Complex. Importantly, the level of 3 ,4 5 show prominent peaks and valleys of QRS-Complex for ease of extraction [33]. See Fig.4 for details.

Peak detection function, which is widely established, commences with the detection of R-Peak as it is the most prominent. In situations of anomaly detection due to the presence of spikes between successive R-Peaks, the algorithm was enhanced with determination of peak-to-peak duration and median duration ranking. This enhancement greatly improved the reliability of R-peak detection in noisy heartwave signal. The detections of the valley peaks namely the Q-Peak and S-Peak were trivial since the two peaks exist about R-Peak. The usually peak/valley detection function is sufficed to perform the detection reliably.

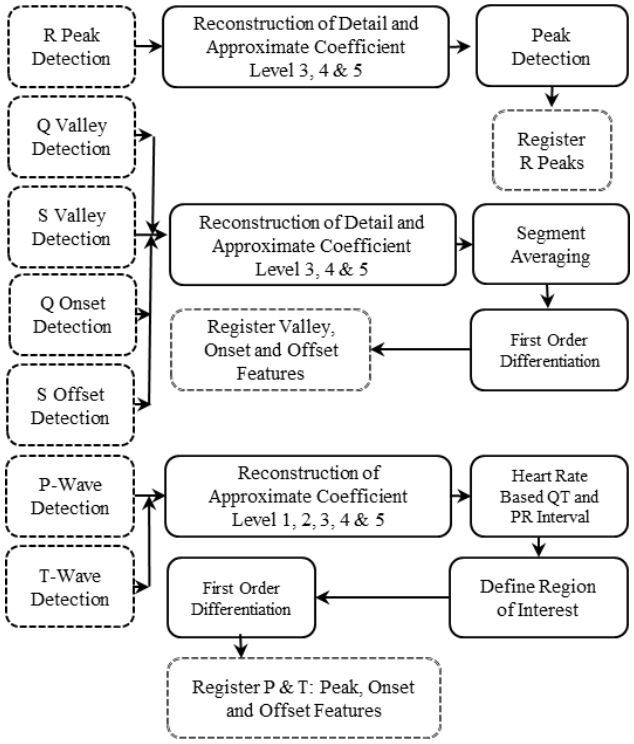

Fig.4. Extraction process sequence of 11 heartwave features

B. T-Wave Features Extraction

A simple and novel method for the detection of T-Wave features uses approximate signals of Level 1, 2, 3, 4 and 5 from Discrete Waveform Transformation. See Fig.3 for details. Frequency spectrum analysis of the combined approximate signals shows clustering of frequencies between 2Hz to 42Hz for full spectrum of heartrate variations.

Under full spectrum of heartrate variation, the time period between R-Peak and T-Wave is inversely proportional to heartrate. A dynamic and adaptive region of interest window that is dependent on the heart rate of the individual was adopted to enable the detection of the local maxima. See Fig.3 for details. The heart rate dependent window takes reference using the QT interval which is defined from the onset of Q-Wave and terminates at the offset of T-Wave. QT interval duration is inversely proportional to the heart rate. The region of interest, based on QT Interval Duration is derived from the QT Interval Nomogram [34, 35] which is a clinical risk assessment tool that predicts risk of QT prolongation in individual in respond to cardiac related drugs. Correct QT formulas such as Bazett or Fredericia are not applicable as they are used to estimate measured QT period to a corrected QTc period based on a heartrate of 60 bpm. The region of interest of QT Interval Duration in accordance to QT Nomogram [34] is valid for heart rate between 64bpm to 154 bpm as shown in (1).

$$QT\ Duration\ (msec) = 2.2095 \times HR\_BPM + 627.41 \quad (1)$$

For heart rate below 64bpm, a constant QT Duration of 484msec was defined. Thereafter, a local maximum was performed to detect the T-Wave peak, offset and onset.

C. P-Wave Features Extraction

The detection of P-Wave features is similar to the detection of T-Wave features where an adaptive region of interest for detection of P-Wave was adopted. See Fig.4 for details.

Table I. Extractions of heartwave from 16 users of different durations

S/N	User	Min Heartrate	Max Heartrate	Duration	No of Heartwave
1	300	91	120	24'50''	2257
2	301	56	133	32'00''	2059
3	302	53	133	23'40''	1834
4	304	51	84	30'20''	1488
5	307	52	103	36'40''	2009
6	309	76	177	41'30''	4650
7	310	89	182	19'00''	2180
8	311	73	159	30'20''	2630
9	312	59	144	27'50''	1984
10	313	65	185	23'00''	2404
11	316	81	189	25'40''	2935
12	320	77	161	32'10''	2746
13	321	70	134	23'00''	1838
14	322	89	137	13'20''	1344
15	325	59	82	21'10''	1210
16	327	54	82	19'50''	1028

As P-Wave resides on the left portion of the R-peak, the region of interest utilizes the PR Interval Duration parameter which varies according to the rate of the heart rate. According to medical definition, PR Interval is defined from the onset of P-Wave till the onset of Q-Wave. The region of interest is defined using the equation developed by [36] which is valid for range of heart rate between 60 bpm to 160 bpm.

$$PR\ Interval\ (msec) = -0.351 \times HR_{BPM} + 176.7 \quad (2)$$

Upon the determination of region of interest for detection, local maxima and minima detection are employed to facilitate the detection of the P-Wave features.

Using the proposed features extraction algorithm, more than 35,000 heartwaves from 16 users were successfully extracted. Although 11 characteristic features are extraction, it is unfortunate that only R-Peak annotation is available. The detected R-Peak is compared against annotated R-Peak. The detection accuracy of R-peak is 99.9% accuracy. The validity of the other 10 characteristic features is visually determined. Due to the sheer size of the heartwave signal, approximately 300 samples are manually determined and the results of the sensitivity have been summarized in the chart below. Each of the detected 10 characteristic features is individually ascertained based on the understanding of the ECG morphology[33]. Concurrently, another of set of sample consisting of approximately 100 heartwaves are validated by a certified medical expert. See Fig. 5 and Table I for details for results of the features validation.

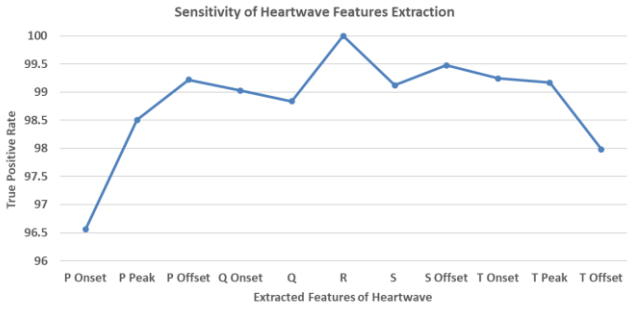

Fig.5. shows the sensitivity of the detected features

III. Data Preparation for Classification

Following the extraction, work was focus towards the classification of the data to support biometric classification using hybridized Generative Model Classifier (GMM+HMM). To maintain consistency in the classification development, only Lead I and Lead II signals will be used for the development of classification algorithm.

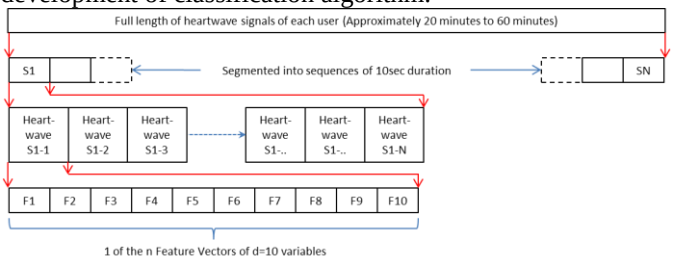

Fig.6. Organization of data to support GMM-HMM classification

In the data preparation, the data from each individual was segmented into multiple sequences of 10 seconds. Each of the sequences can contain from 8 to as much as 30 individual segmented sequential heartwaves which is proportional to the heartrate acquired at that instance. Please see Fig.6 for illustration of data preparation. The segmented sequences are subsequently used for classification development via Mixture Gaussian Model with Hidden Markov Method.

IV. Classification Methodology

A. User Specific Gaussian Mixture Model

With the understanding of the heartwave morphological changes in a single session of treadmill exercise, the heartwave feature vector comprising of 11 fiducial parameters can be normally distributed into different components signifying different states of heartwave signals. GMM is used to classify all the heartwave signals from each individual into respective components using k-means clustering.

For each user, all the individual heartwaves are concatenated to form an array of observations in rows by 11 fiducial parameters as columned in the format of [m x d]. The optimization using Gaussian Mixture Model (GMM) begins with the observation probability:

$$p(x_i|\theta_i) = \sum_{k=1}^{K_i} \pi_{ik} \mathcal{N}(x_i|\mu_{ik}, \Sigma_{ik}) \quad (3)$$

where $p(x_i|\theta_i)$ refers to the probability density function of a mixture model, $\mathcal{N}(x_i|\mu_{ik}, \Sigma_{ik})$ as the Gaussian distribution and π_{ik} as the weightage.

In mixture of Gaussian, each of the heartwave signal has a probability of belonging to the respective components and hence can be computed as follow.

$$w_{ik} = p(z_{ik} = 1|x_i, \theta_{ik}) = \frac{p(x_i|z_{ik},\theta_{ik})\ \alpha_{ik}}{\sum_{m=1}^{K} p(x_i|z_{m},\theta_{im})\ \alpha_{im}} \quad (4)$$

where $\theta_{ik} = (\pi_{ik}, \mu_{ik}, \Sigma_{ik})$ contains the parameters for each of the components for each user subscripted by i. α_{ik} represents the mixing weightage relatives to the components. μ_{ik} and Σ_{ik} are the mean and covariance relatives to the components. K is the number of components for specific Gaussian Mixture Model. Using Expectation Maximization (EM) approach, an optimized GMM model for each user was achieved. EM algorithm comprises of 2 steps: E-Step and M-Step. E-Step estimates the probability of each data point belonging to each of the clusters or components. Thereafter, the estimated distribution is fed into M-Step to maximize the joint distribution and the hidden variable. The process is iterative and stopped until the change in loglikelihood is less than $1x10^{-5}$ difference. The parameters are updated using the equations:

$$\hat{\mu}_{ik} = \frac{1}{n_k} \sum_i^n p(w_{ik}|x_i, \theta_{ik}) x_i \quad (5)$$

$$\hat{\Sigma}_{ik} = \frac{1}{n_k} \sum_{i=1}^n p(w_{ik}|x_i, \theta_{ik})(x_i - \hat{\mu}_{ik})(x_i - \hat{\mu}_{ik})^T \quad (6)$$

$$\hat{\pi}_{ik} = \frac{n_k}{n} \quad (7)$$

where $n_k = \sum_i^n p(w_{ik}|x_i, \theta_{ik})$. The loglikelihood which computed based on original parameters for the entire data is given by

$$L_\theta = \log p(x_i|\mu_{ik}, \Sigma_{ik}) = \sum_{i=1}^n \left(log \sum_{k=1}^K \pi_{ik}\, \mathcal{N}(x_i|\mu_{ik}, \Sigma_{ik})\right) \quad (8)$$

The characteristic of GMM has the tendency to approach positive loglikelihood score at higher components. Hence, the process to limit the number of components was executed to minimize over-fitting. Bayesian Information Criterion (BIC) and Minimum Description Length (MDL) were implemented via imposing a penalty term to the loglikelihood result. Both BIC and MDL are for true models as they account for the data and more explicitly, MDL accounts for total number of data values. This allows MDL to impose a heavier penalty for more complex model as compared to BIC estimation [37, 38]. The equations for BIC and MDL are as follow shown in (10) and (11).

$$BIC(K,\theta) = -2\sum_{i=1}^{n} \log p(x_i|\theta_i)^{ML} + L\log(n) \quad (10)$$

$$MDL(K,\theta) = -\sum_{i=1}^{n} \log p(x_i|\theta_i)^{ML} + (L/2)\log(dn) \quad (11)$$

where $= K\left(1 + d + \frac{d(d+1)}{2}\right) - 1$, d is the number of features, n is the number of data values, K is the number of components.

Table II shows the component limits for each users. Most of the users have an optimum component at approximately 20. User_311 did not achieve optimum component using BIC Criterion unless the range of components testing is extended. Using MDL however was able to establish the optimum component at 25. The table also shows similar optimum components for both BIC Criterion and MDL for most users.

Table II: Component limit for each user in GMM modelling

S/N	User	Min HR	Max HR	No of Sequences	BIC	MDL
1	300	91	120	149	19	19
2	301	56	133	190	19	19
3	302	53	133	142	16	16
4	304	51	84	182	18	14
5	307	52	103	219	20	19
6	309	76	177	249	23	23
7	310	89	182	114	18	18
8	311	73	159	182	0	24
9	312	59	144	166	23	23
10	313	65	185	138	21	18
11	316	81	189	150	15	15
12	320	77	161	193	21	21
13	321	70	134	138	23	17
14	322	89	137	80	12	12
15	325	59	82	127	13	13
16	327	54	82	119	21	21

B. User Specific Hidden Markov Model (HMM)

With GMM model derived for each individual to represent the full spectrum of heartwave morphologies, the next stage is the generation of HMM model for each individual. In every dataset of sequences, the heartwave can exist at any stationary state or any series of state sequence. For example, during the recovery from strenuous exercise, an individual heartrate can progress from a heartrate of 120bpm to a recovery heartrate of 90bpm within a span of 2 minutes. HMM will thus be able to statistically determine the progression of states given a sequence or concatenated sequences.

In the generation of HMM for each user, every model of each individual will have a model parameter represented by$\lambda_{user,k}$. The $\lambda_{user,k}$ comprises of $(\boldsymbol{A},\boldsymbol{B},\Pi)$ where A is the state transition probability distribution$\{a_{ij}\}$, B is the observation probability distribution $\{b_i(v_k)\}$ where v is the symbol observation at the respective state and Π as the initial state distribution. In the GMM model generation for individual user, the number of components necessary to represent the entire morphological changes is limited by using Bayesian Information Criterion (BIC) and Minimum Description Length (MDL) which is estimated at 25. Hence, in the HMM construction, it is important to determine the number of state necessary to provide a reliable classification. This paper uses the limiting components to represent the number of states required in the initial state. Each state will be the distribution probability for each of GMM components.

For the computation of the HMM model for each user, forward and backward algorithm are determined. For each of the nodes, the forward algorithm is given by

$$\alpha_{t+1}(j) = \left[\sum_{i=1}^{k} \alpha_t(i)a_{ij}\right].b_{ij}(O_t) \quad (12)$$

$$P(O|\lambda) = \sum_{i=1}^{k} \alpha_t(T) \quad (13)$$

where a_{ij} and $b_{ij}(O_t)$ are the initialized transmission probability (ergodic topology) and emission probability via means and covariance. Similarly, at the reverse order, backward algorithm is used:

$$\beta_t(i) = \sum_{j=1}^{k} a_{ij}b_j(O_{t+1})\,\beta_{(t+1)}(j) \quad (14)$$

Thereafter the state probability where the process was in state i at time t and normalized by the total number of states at given t was computed

$$\gamma_i(t) = \frac{\alpha_t(i)\beta_t(i)}{\sum_{i=1}^{k} \alpha_t(T)} \quad (15)$$

Following, probability of the sequence at state *i* at time *t* and state *j* at time *t*+1 was computed using

$$\xi_{ij}(t) = \frac{\alpha_i(t)a_{ij}b_j(O_{t+1})\beta_j(t+1)}{\sum_{i=1}^{k} \alpha_t(T)} \quad (16)$$

Thereafter, the following parameters were updated to test for observation convergence

$$a_{ij} = \frac{\sum_{t=1}^{T-1} \alpha_i(t)a_{ij}b_j(O_{t+1})\beta_j(t+1)}{\sum_{t=1}^{T-1} \alpha_t(i)\beta_t(i)} \quad (17)$$

$$\hat{\mu} = \frac{\sum_{t=1}^{T} \gamma_i(t)O_t}{\sum_{t=1}^{T} \gamma_i(t)} \quad (18)$$

$$\Sigma_i = \frac{\sum_{t=1}^{T} \gamma_i(t)(O_t-\hat{\mu})(O_t-\hat{\mu})^T}{\sum_{t=1}^{T} \gamma_i(t)} \quad (19)$$

The probabilities of the observation are recomputed using the updated HMM parameters if the loglikelihood score does not converge.

V. Experimentation and Results

A. Parameters Optimization

1) Parameters Optimization: Size of Data for Training

The percentage of data necessary to train a GMM-HMM was examined to ensure that the identification performance will be at optimum as it is not practical to train HMM model based on all data and at the same time to continuously train HMM upon an addition of new data. This investigation uses the results of loglikelihood as a criteria to determine to most appropriate proportion of data for training.

For each individual, the size of the training dataset started off with percentage of data for training from 10% to 100%. Sequences not using in the training of HMM model are used to

determine the loglikelihood score. The selection of the sequences for training are randomly generated. Fig.7 shows the distribution of the loglikelihood score from User316. Notice that the loglikelihood scores were homogenous at the heartrate of 120bpm and below. When the heartrate was between 140bpm to 180bpm, the loglikelihood scores were in the range between -600 to -1000. This is attributed to the morphological changes in the heartwave signal where the heart went into supraventricular tachycardia mode.

The results from each individual was average and normalized with the average score at 10% point. Fig.8 shows the distribution of normalized loglikelihood for each individual. Using 10% to 20% of data sequences for training has a tendency to under-fit which leads to higher means and standard deviations. Conversely, having too much data for training will lead to a situation of over-fit as evident from the Fig.8. Hence, a stable region will be within the range of 40% to 70% which can be appropriate for HMM parameter training. This work uses the upper bound of 70% for a more conservative approach which is also aligned with report works.

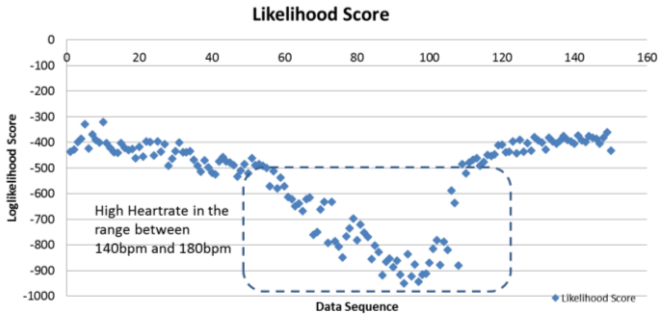

Fig.7. Distribution of loglikelihood score from an individual with its own data sequences

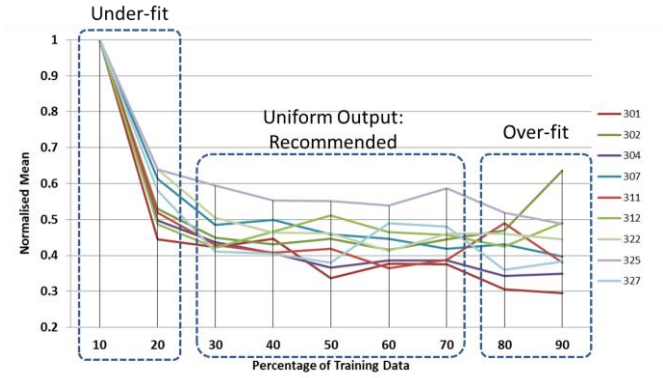

Fig.8. Distribution of normalized mean scores at increasing training data

2) Parameters Optimization: GMM-HMM State Optimization

In the GMM model generation of individual user, the number of components to represent the entire morphological changes is limited by using Bayesian Information Criterion (BIC) and Minimum Description Length (MDL) which is estimated at 25. Hence, to effectively determine the states required for GMM-HMM classification, 25 sub-models for each user were created. Simply, each user will have 25 HMM models ranging from HMM model with 1 state to model with 25 states. Optimization is performed to determine the optimal number of states for identification.

With 70% of data as training data, a total of 786 test sequences from all users are used to perform classification. The 786 test sequences are tested on all HMM models. For each test sequence, the user specific HMM model that outputs the maximum loglikelihood result was indexed and tabulated. The results were tabulated using confusion table for each of 25 states before being summarized into Fig.9 and Fig.10.

Fig.9 shows the Sensitivity analysis which is the ability to authorize access to the correct users. It shows that Sensitivity achieved well over 90% at lower states between State 1 and State 5 under the worst case scenario. This aligns well with the objectives that BIC and MDL criterion were useful to limit over-specification and conserve computation processing.

Fig.9 also shows the Specificity analysis which is defined as ability to deny access to unauthorized individuals. The results of the Specificity for all 25 states were impressive as the specificity were well above 90% for all levels of states. While the sensitivity and specificity have shown impressive results, the False Positive and False Negative in contrast provided avenues for more robust investigation.

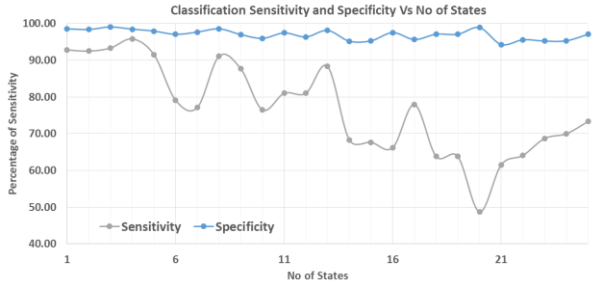

Fig.9 Sensitivity and Specificity results of GMM-HMM classification for 25 different states.

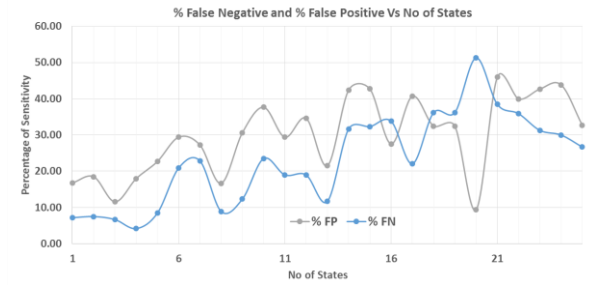

Fig.10. Percentage of False Positive and False Negative of GMM-HMM classification for 25 different states

Fig.10 shows the False Positive results at different states. At lower states of up to State 4, the False Positive is 20% and below. Beyond State 4, the False Positive Errors were excess of 20% exclude State 8 and State 20.

In the False Negative results where authorized individuals were denied access, the False Negative errors were below 10% at State 5 and below. Based on best fit, the error worsens at increasing number of States. This observation is in-line with results of False Positive and Sensitivity that lower states provide better classification results. Thus this analysis concluded that low number states up to 5 states, offers the most appropriate selection without compromising the results.

B. Classification

1) User Classification With User-Specific Thresholding

Recap in Fig. 9 and Fig. 10, where the classification is

based on the maximum likelihood score, it is not practical to use a model generated score to perform classification in particular when the population grows too big. An important observation is the presence of user specific parameters maximum and median loglikelihood scores. See Fig. 11 for user specific score. Due to the nature of individual physiological signals, the user specific thresholding criteria on median loglikelihood score can be used to classify users.

In this validation, all individual's 30% of the untrained data sequences are input as a lot to all the user specific GMM-HMM model to perform classification. The criteria to classify each sequence is dependent on user specific thresholding criteria of median loglikelihood score.

The results were tabulated and represented in ROC as shown in Fig. 11. The results using user specific median threshold value achieved a 68% True Positive Rate with a corresponding 10% False Positive Negative Rate. Compared to using maximum loglikehood score, the False Positive Rate improved by double to achieve a False Positive Rate of 10%

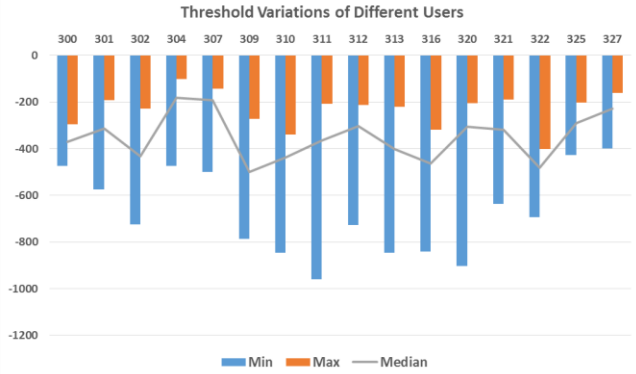

Fig.11. Distribution of the different thresholds: Minimum, Maximum and Median from all users

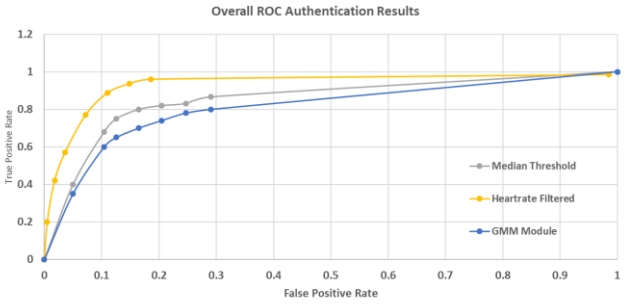

Fig.12. Relative Operating Characteristic of the identification process using median threshold, proposed architecture and GMM Module only.

2) Classification With User-Specific Heartrate and Thresholding Criteria

To further improve the classification, the use of individual heartrate in the identification process is proposed. Every individual has confined range of heartrate between resting and maximum duress. Hence, the individual likelihood score is constructed against individual heartrate. The plot of heartrate vs likelihood score provides a unique criteria score for each individual. The likelihood score from GMM-HMM is compared against user specific criteria score.

Through the use of heartrate in the classification, the identification improves by more than 35% to achieve a 0.89 True Positive Rate while maintaining a False Positive Rate of 0.11. Fig. 13 shows the performance comparison between proposed architecture and fiducial based Linear Discriminant Analysis (LDA) with Nearest Center as classifier. The LDA is commonly used in machine learning for biometrics verification and identification. To enable fair comparison with the LDA methodology, similar database from the proposed method is used. The performance of LDA achieved a TPR of approximately 0.78 and FPR of 0.25. In another comparison, GMM-HMM with user specific median score as criteria achieved 0.68 for TPR and 0.11 for FPR. This reinforces the hypothesis that the use of heartrate together with user specific thresholding criteria is crucial to achieve better identification accuracy under highly variated heartwave signals.

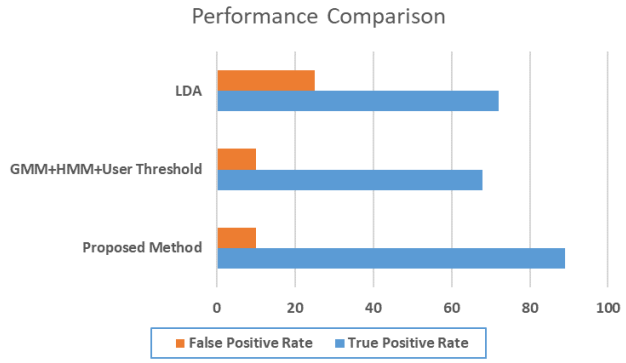

Fig.13. Performance comparison of proposed method with LDA and user-specific heartrate GMM-HMM methods

3) Impact of Performance Between Resting and Intense Heartrate

The effect of heartwave morphological changes from heartrate variation (rest state to intense duress state) on the performance of the proposed architecture is investigated. Resting heartrates from all users are sorted and tested on the proposed architecture, and compared against the LDA and GMM-only module (excluding the HMM) approaches. Using resting heartrate dataset, the EER for the proposed architecture and LDA approach are relatively similar at 0.03 and 0.035 respectively. However, with the inclusion of heartwave data under intense heartrate, the EER for proposed architecture and LDA approach are 0.11 and 0.25 respectively. The performance of the proposed architecture has performed reasonably well at EER 0.11 on heartwave signal under full spectrum of heartrate variation. The result is shown in Fig. 14.

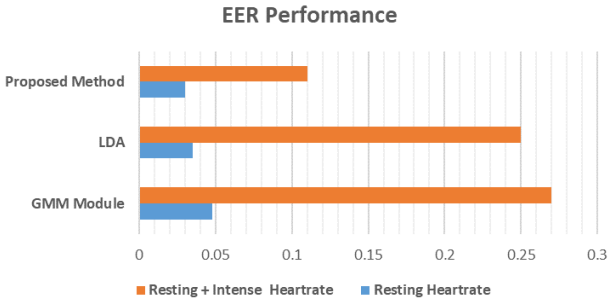

Fig.14. Comparison of proposed method against fiducial based LDA and GMM

VI. Conclusion

The identification of individuals using heartwave has shown promising results. In the extraction process, it has proven that the use of heartrate adaptive parameters such as QT interval from Nomogram and PR interval have led to reliable extractions of heartwave features. In the preparation of data for classification, it is concluded that the use of BIC and MDL to limit the components do not significantly contribute to better classification results. In GMM-HMM classification testing, results have shown that the classification performs better at lower number of states than in higher number of states. The classification work to support identification achieved an ERR of 0.11.

It has been shown that using User-Specific Heartrate and Thresholding Criterial yielded a much desirable performance. Deliberately, identification performance is performed with just the GMM module using the same dataset. The EER based on GMM module alone is approximately 0.27. This underlines the importance of HMM module to achieve better identification performance. The work is limited by the availability of heartwave data where user has been subjected to physiological duress. However at the current development, the results have shown the feasibility of using heartwave signal as biometric mode with varying heartrate. This work has demonstrated that at varying heartrate, the heartwave signal exhibited unique characteristic features that can be used to discriminate individual.

References

[1] S. A. Israel, J. M. Irvine, A. Cheng, M. D. Wiederhold, and B. K. Wiederhold, "ECG to identify individuals," *Pattern Recognition*, vol. 38, pp. 133-142, 2005.

[2] L. Biel, O. Pettersson, L. Philipson, and P. Wide, "ECG analysis: a new approach in human identification," *IEEE Transactions on Instrumentation and Measurement*, vol. 50, pp. 808-812, 2001.

[3] Y. Si, J. Mei, and H. Gao, "Novel Approaches to Improve Robustness, Accuracy and Rapidity of Iris Recognition Systems," *IEEE Transactions on Industrial Informatics*, vol. 8, pp. 110-117, 2012.

[4] M. A. M. Abdullah, S. S. Dlay, W. L. Woo, and J. A. Chambers, "A novel framework for cross-spectral iris matching," *IPSJ Transactions on Computer Vision and Applications*, vol. 8, p. 9, November 05 2016.

[5] M. A. M. Abdullah, S. S. Dlay, W. L. Woo, and J. A. Chambers, "Robust Iris Segmentation Method Based on a New Active Contour Force With a Noncircular Normalization," *IEEE Transactions on Systems, Man, and Cybernetics: Systems*, vol. 47, pp. 3128-3141, 2017.

[6] S. Alkassar, W. L. Woo, S. S. Dlay, and J. A. Chambers, "Robust Sclera Recognition System With Novel Sclera Segmentation and Validation Techniques," *IEEE Transactions on Systems, Man, and Cybernetics: Systems*, vol. 47, pp. 474-486, 2017.

[7] S. Alkassar, W. L. Woo, S. Dlay, and J. Chambers, "Sclera recognition: on the quality measure and segmentation of degraded images captured under relaxed imaging conditions," *IET Biometrics*, vol. 6, pp. 266-275, 2017.

[8] M. S. Hossain, G. Muhammad, S. M. M. Rahman, W. Abdul, A. Alelaiwi, and A. Alamri, "Toward end-to-end biomet rics-based security for IoT infrastructure," *IEEE Wireless Communications*, vol. 23, pp. 44-51, 2016.

[9] S. Izumi, K. Yamashita, M. Nakano, S. Yoshimoto, T. Nakagawa, Y. Nakai, *et al.*, "Normally Off ECG SoC With Non-Volatile MCU and Noise Tolerant Heartbeat Detector," *IEEE Transactions on Biomedical Circuits and Systems*, vol. 9, pp. 641-651, 2015.

[10] M. I. Ahmad, W. L. Woo, and S. Dlay, "Non-stationary feature fusion of face and palmprint multimodal biometrics," *Neurocomputing*, vol. 177, pp. 49-61, 2016/02/12/ 2016.

[11] R. R. O. Al-Nima, S. S. Dlay, S. A. M. Al-Sumaidaee, W. L. Woo, and J. A. Chambers, "Robust feature extraction and salvage schemes for finger texture based biometrics," *IET Biometrics*, vol. 6, pp. 43-52, 2017.

[12] K. T. Chui, K. F. Tsang, H. R. Chi, B. W. K. Ling, and C. K. Wu, "An Accurate ECG-Based Transportation Safety Drowsiness Detection Scheme," *IEEE Transactions on Industrial Informatics*, vol. 12, pp. 1438-1452, 2016.

[13] G. Yang, L. Xie, M. Mäntysalo, X. Zhou, Z. Pang, L. D. Xu, *et al.*, "A Health-IoT Platform Based on the Integration of Intelligent Packaging, Unobtrusive Bio-Sensor, and Intelligent Medicine Box," *IEEE Transactions on Industrial Informatics*, vol. 10, pp. 2180-2191, 2014.

[14] G. R. Shaw and P. Savard, "On the detection of QRS variations in the ECG," *IEEE Trans Biomed Eng*, vol. 42, pp. 736-41, Jul 1995.

[15] L. S. Green, R. L. Lux, C. W. Haws, R. R. Williams, S. C. Hunt, and M. J. Burgess, "Effects of age, sex, and body habitus on QRS and ST-T potential maps of 1100 normal subjects [published erratum appears in Circulation 1986 Oct;74(4):785]," *Circulation*, vol. 71, pp. 244-253, 1985.

[16] F. Agrafioti and D. Hatzinakos, "Signal validation for cardiac biometrics," in *2010 IEEE International Conference on Acoustics, Speech and Signal Processing*, 2010, pp. 1734-1737.

[17] M. Homer, J. M. Irvine, and S. Wendelken, "A model-based approach to human identification using ECG," 2009, pp. 730625-730625-10.

[18] I. Odinaka, L. Po-Hsiang, A. D. Kaplan, J. A. O'Sullivan, E. J. Sirevaag, and J. W. Rohrbaugh, "ECG Biometric Recognition: A Comparative Analysis," *Information Forensics and Security, IEEE Transactions on*, vol. 7, pp. 1812-1824, 2012.

[19] K. A. Sidek, I. Khalil, and M. Smolen, "ECG biometric recognition in different physiological conditions using robust normalized QRS complexes," in *Computing in Cardiology (CinC), 2012*, 2012, pp. 97-100.

[20] K. Kyeong-Seop, Y. Tae-Ho, L. Jeong-Whan, K. Dong-Jun, and K. Heung-Seo, "A Robust Human Identification by Normalized Time-Domain Features of Electrocardiogram," in *Engineering in Medicine and Biology Society, 2005. IEEE-EMBS 2005. 27th Annual International Conference of the*, 2005, pp. 1114-1117.

[21] P. Shing-Tai, W. Yi-Heng, K. Yi-Lan, and C. Hung-Chin, "Heartbeat Recognition from ECG Signals Using Hidden Markov Model with Adaptive Features," in *Software Engineering, Artificial Intelligence, Networking and Parallel/Distributed Computing (SNPD), 2013 14th ACIS International Conference on*, 2013, pp. 586-591.

[22] E. Rabhi and Z. Lachiri, "Biometric personal identification system using the ECG signal," in *Computing in Cardiology Conference (CinC), 2013*, 2013, pp. 507-510.

[23] P. Shing-Tai, H. Tzung-Pei, and C. Hung-Chin, "ECG signal analysis by using Hidden Markov model," in *Fuzzy Theory and it's Applications (iFUZZY), 2012 International Conference on*, 2012, pp. 288-293.

[24] F. Agrafioti and D. Hatzinakos, "ECG biometric analysis in cardiac irregularity conditions," *Signal, Image and Video Processing*, vol. 3, pp. 329-343, 2008.

[25] J. Carlson, R. Johansson, and S. B. Olsson, "Classification of electrocardiographic P-wave morphology," *Biomedical Engineering, IEEE Transactions on*, vol. 48, pp. 401-405, 2001.

[26] R. Rodríguez, A. Mexicano, J. Bila, S. Cervantes, and R. Ponce, "Feature Extraction of Electrocardiogram Signals by Applying Adaptive Threshold and Principal Component Analysis," *Journal of Applied Research and Technology*, vol. 13, pp. 261-269, 2015/04/01/ 2015.

[27] C. L. P. Lim, W. L. Woo, and S. S. Dlay, "Enhanced wavelet transformation for feature extraction in highly variated ECG signal," in *2nd IET International Conference on Intelligent Signal Processing 2015 (ISP)*, 2015, pp. 1-6.

[28] M. Niknazar, B. V. Vahdat, and S. R. Mousavi, "Detection of characteristic points of ECG using quadratic spline wavelet transfrom," in *Signals, Circuits and Systems (SCS), 2009 3rd International Conference on*, 2009, pp. 1-6.

[29] D. Sadhukhan and M. Mitra, "Detection of ECG characteristic features using slope thresholding and relative magnitude comparison," in *Emerging Applications of Information Technology (EAIT), 2012 Third International Conference on*, 2012, pp. 122-126.

[30] S. Pal and M. Mitra, "Detection of ECG characteristic points using Multiresolution Wavelet Analysis based Selective Coefficient Method," *Measurement*, vol. 43, pp. 255-261, 2010.

[31] P. R. Gomes, F. O. Soares, J. H. Correia, and C. S. Lima, "ECG Data-Acquisition and classification system by using wavelet-domain Hidden Markov Models," in *Engineering in Medicine and Biology Society (EMBC), 2010 Annual International Conference of the IEEE*, 2010, pp. 4670-4673.

[32] S. Z. Mahmoodabadi, A. Ahmadian, and M. D. Abolhasani, "ECG feature extraction using daubechies wavelets," *5th IASTED International Conference Visualization, Imaging, and Image Processing*, pp. 343-348, September 7-9 2005.

[33] "Recommendations for measurement standards in quantitative electrocardiography. The CSE Working Party," *Eur Heart J*, vol. 6, pp. 815-25, Oct 1985.

[34] A. Chan, G. K. Isbister, C. M. Kirkpatrick, and S. B. Dufful, "Drug-induced QT prolongation and torsades de pointes: evaluation of a QT nomogram," *Qjm*, vol. 100, pp. 609-15, Oct 2007.

[35] A. A. Fossa, T. Wisialowski, A. Magnano, E. Wolfgang, R. Winslow, W. Gorczyca, *et al.*, "Dynamic Beat-to-Beat Modeling of the QT-RR Interval Relationship: Analysis of QT Prolongation during Alterations of Autonomic State versus Human Ether a-go-go-Related Gene Inhibition," *Journal of Pharmacology and Experimental Therapeutics*, vol. 312, pp. 1-11, January 1, 2005 2005.

[36] S. G. Carruthers, B. McCall, B. A. Cordell, and R. Wu, "Relationships between heart rate and PR interval during physiological and pharmacological interventions," *British Journal of Clinical Pharmacology*, vol. 23, pp. 259-265, 1987.

[37] H. Tenmoto, M. Kudo, and M. Shimbo, "MDL-based selection of the number of components in mixture models for pattern classification," in *Advances in Pattern Recognition: Joint IAPR International Workshops SSPR'98 and SPR'98 Sydney, Australia, August 11–13, 1998 Proceedings*, A. Amin, D. Dori, P. Pudil, and H. Freeman, Eds., ed Berlin, Heidelberg: Springer Berlin Heidelberg, 1998, pp. 831-836.

[38] Z. Liu, B. Malone, and C. Yuan, "Empirical evaluation of scoring functions for Bayesian network model selection," *BMC Bioinformatics*, vol. 13, pp. S14-S14, 09/11 2012.

C. L. P. Lim received his B.Eng (Hons) degree in Mechatronics Engineering from University of New South Wales, Australia in 2000. In 2009, he obtained his Dual M.Sc. degrees (Micro Electro Mechanical System, MEMS) from Nanyang Technological University, Singapore and École Supérieure d'Ingénieurs en Électrotechnique et Électronique (ESIEE), France. He is currently working towards his PhD degree at Newcastle University focusing on heartwave based biometric authentication using methodologies of statistical tools and neural network.

W. L. Woo (M'09–SM'11) received the BEng degree in Electrical and Electronics Engineering and the PhD degree from the Newcastle University, UK. He was awarded the IEE Prize and the British Scholarship. He is currently a Reader in Intelligent Signal Processing and Director of Operations for the international branch of the university in Singapore. His major research is in the mathematical theory and algorithms for machine learning and multidimensional signal processing. Dr. Woo is a Member of the Institution Engineering Technology. He was a recipient of the IEE Prize and the British Scholarship. Currently, he serves on the editorial board of the several international signal processing journals.

S. S. Dlay received his BSc (Hons.) degree in Electrical and Electronic Engineering and his PhD in VLSI Design from the Newcastle University. During this time he held a Scholarship from the Engineering and Physical Science Research Council (EPSRC) and the Charles Hertzmann Award. In 1984 he was appointed as a Lecturer in the Department of Electronic Systems Engineering at the University of Essex. In 1986 he re-joined the Newcastle University as a Lecturer, then in 2006 he was appointed to a Personal Chair in Signal Processing Analysis. Professor Dlay is a College Member of the EPSRC.

Bin Gao (M' 12-SM' 14) received his B.S. degree in communications and signal processing from Southwest Jiao Tong University (2001-2005), China, MSc degree in communications and signal processing with Distinction and PhD degree from Newcastle University, UK (2006-2011). His research interests include sensor signal processing, machine learning, nondestructive testing and evaluation. Currently, he is a Professor with the School of Automation Engineering, University of Electronic Science and Technology of China (UESTC), Chengdu, China.